Precision surface characterization for finish cylindrical milling with dynamic tool displacements model

S. Wojciechowski [1], P. Twardowski [1], M. Pelic [1], R. W. Maruda [2], S. Barrans [3], G.M. Krolczyk[4]

[1] Faculty of Mechanical Engineering and Management, Poznan University of Technology,
3 Piotrowo St., 60-965 Poznan, Poland, email: sjwojciechowski@o2.pl
[2] Faculty of Mechanical Engineering, University of Zielona Gora,
4 Prof. Z. Szafrana Street, 65-516 Zielona Gora, Poland, email: r.maruda@ibem.uz.zgora.pl
[3] Turbocharger Research Institute, University of Huddersfield,
Huddersfield HD1 3DH, UK, email: s.m.barrans@hud.ac.uk
[4] Corresponding author: Faculty of Mechanical Engineering, Opole University of Technology,
76 Proszkowska St., 45-758 Opole, Poland, email: g.krolczyk@po.opole.pl,

Abstract

This paper presents a novel approach to surface roughness parameter estimation during finish cylindrical end milling. The proposed model includes the influence of cutting parameters, the tool's static run out and dynamic phenomena related to instantaneous tool deflections. The modeling procedure consists of two parts. In the first stage, tool working part instantaneous displacements are estimated using an analytical model which considers tool dynamic deflections and static errors of the machine – tool-holder - tool system. The obtained height of the tool's displacement envelope is then applied in the second stage to the calculation of surface roughness parameters. These calculations assume that in the cylindrical milling process, two different mechanisms of surface profile formation exist. Which mechanism is present is dependent on the feed per tooth and the maximum height of the tool's displacement envelope. The developed model is validated during cylindrical milling of hardened hot-work tool steel 55NiCrMoV6 using a stylus profiler and scanning laser vibrometer over a range of cutting parameters. The surface roughness values predicted by the developed model are in good agreement with measured values. It is shown that the application of a model which includes only the effect of static displacements gives an inferior estimation of surface roughness compared to the model incorporating dynamic tool deflections.

Keywords

finish milling; tool displacement; run out; surface roughness; laser vibrometry

1 Introduction

Milling of difficult to cut materials in a hardened state is an efficient technology which is usually applied to the production of drop forging dies and casting molds [1, 2]. This machining technique is very often carried out to generate parts in the finished condition, which consequently imposes high dimensional accuracy and low surface roughness constraints on the process. The improvement of machined surface quality is a very important task, because it has direct influence on performance and tribological properties of product [3, 4]. Fulfilling the demanding surface quality requirements depends mainly on the machine – tool-holder - tool system's condition and appropriate selection of milling parameters. Selection of appropriate milling parameters and constraints on the machine tool accuracy requires the application of a reliable and versatile surface roughness model.

According to Twardowski et al. [5], during cylindrical milling of hardened steel 55NiCrMoV6, the measured surface roughness parameters are significantly higher than theoretical values resulting from a kinematic-geometric model. These differences can be caused by the tribological phenomena in the tool-work material interface (e.g. tool's micro-geometry, wear, lubrication) [6], plastic deformations of work material during de-cohesion, loss of process stability and tool displacements [7]. Thus, the complexity of the surface formation mechanism during milling has resulted in many modeling approaches. The proposed models usually include kinematic-geometric parameters, insert setting errors, radial and axial run outs and static tool deflections. Baek et al. [8] formulated a surface roughness model for the face milling process considering cutter insert run out errors and feed-rate. The verification results confirmed that the proposed model was valid for controlling the surface roughness and maximizing the material removal rate. Li et al. [9] established a surface generation model for the end milling process accounting for movement error of the principle rotation axis and the tool's static stiffness. It was concluded that tooth point curve radius significantly affects the height of surface roughness. Franco et al. [10] proposed a theoretical surface profile model for face milling including back cutting surface marks and run out phenomenon. Research revealed that surface roughness parameters *Ra* and *Rt* can be minimized by reducing back cutting height deviation. Buj-Corral et al. [11] developed a surface topography model for peripheral milling incorporating feed per tooth, radius of each cutting tooth, tool eccentricity and helix angle. It was noticed that the roughness profiles varied along the work piece's height when eccentricity was present and tools with non-zero helix angles were used.

The application of the above-mentioned models improves the accuracy of the surface roughness estimation. However, during the machining process, surface texture can be affected also by the tool's dynamic displacements, which are caused by an instantaneous cutting forces and geometrical errors of the milling system. Thus, Baek et al. [12] formulated a dynamic surface roughness model for face milling, which considers cutting conditions, edge profiles and relative displacements between the work-piece and the cutting tool. A similar dynamic modeling approach, proposed by Zhenyu et al. [13] focused on surface roughness estimation during high speed face milling with straight-edged square inserts. Peigne et al. [14] developed a dynamic deflection model for surface roughness estimation during peripheral milling. The proposed system was of the rigid cutter - flexible work-piece type. Liu and Cheng [15] also formulated a dynamic surface roughness model for peripheral milling. However their approach was based on a 4 degrees of freedom dynamic model with a flexible tool and work-piece. Schmitz et al. [16] applied the "Regenerative Force, Dynamic Deflection Model" for the estimation of surface finish, surface location error and stability during the end milling process. Furthermore, previous research by Wojciechowski [17] related to cylindrical milling of hardened steel revealed that the application of a dynamic displacement model significantly increases the accuracy of roughness parameter estimation, in comparison to a traditional kinematic-geometric model.

Models which describe a tool's instantaneous displacements and the influence on surface roughness require reliable validation. However, this is inhibited by the difficulty of directly measuring the tool's dynamic displacement during milling. Therefore, the displacements are usually measured indirectly with the application of accelerometers fixed to the spindle head or work-piece. However, the acquired signal requires further processing (integration and filtration) and may not accurately represent the true tool displacement. Thus, novel, non-contact measurement methods of instantaneous tool displacements are being developed. These approaches are based on the application of laser vibrometry [18], capacitive gap sensors [19], or laser displacement sensors [20].

The state of the art shows that surface formation during milling is affected both by static phenomena (kinematic-geometric parameters, insert setting errors, run out, static tool deflections) and dynamic tool displacements. However, the majority of works related to surface roughness modeling do not include these factors simultaneously. Therefore, this paper proposes a versatile surface roughness

model for the cylindrical milling which includes the influence of cutting parameters, tool static radial run out, and deflections induced by cutting forces. The developed model is validated experimentally using a stylus profiler and scanning laser vibrometer, over a range of variable cutting parameters.

2 SURFACE ROUGHNESS MODEL INCLUDING CUTTER'S DISPLACEMENTS IN CYLINDRICAL MILLING

Theoretic surface roughness values calculated for the cylindrical milling process, on the basis of models including only kinematic-geometric parameters often vary from the real surface roughness values, especially for low feeds. One of the most important reasons of these discrepancies are cutter displacements.

Based on the conclusions from earlier investigations [20] a displacement model has been developed. This approach refers to the case when the milling tool rotates around the spindle axis with an eccentricity and is considered as a dynamic system with 1 degree of freedom. Therefore, the cutter's working part displacements are caused by the static radial run out e_r and deflections induced by the cutting forces (see – Fig. 1). The proposed model considers only the displacements which are perpendicular to the machined surface, because of their direct influence on the surface profile formation.

The instantaneous value of total tool displacement can be calculated from the equation:

$$y(t) = y_r(t) + y_d(t) \tag{1}$$

where: $y_r(t)$ is the instantaneous partial tool working part displacement caused by static radial run-out, $y_d(t)$ is the instantaneous partial tool working part deflection caused by cutting forces and $y(t)$ is the instantaneous total tool working part displacement.

The instantaneous partial tool working part displacement caused by static radial run out can be expressed as:

$$y_r(t) = -(e_r) \cdot \cos\left[\Omega + \delta - \frac{1}{2}\left(\pi + \frac{a_p \cdot \tan\lambda_s}{R} - \psi\right)\right] \tag{2}$$

where: Ω is the tool rotation angle [rad], δ is the radial run out angle [rad], ψ is the tool working angle [rad], λ_s is the tool major cutting edge inclination angle, R is the tool radius and a_p is the axial depth of cut [mm].

The tool rotational Ω and working angle ψ are described by the following equations:

$$\Omega = \frac{\pi \cdot n \cdot t}{30} \tag{3}$$

$$\psi = \arccos\left(1 - \frac{a_e}{R}\right) \tag{4}$$

where: n is the spindle rotational speed [rev/min], t is time [s] and a_e is the radial depth of cut [mm].

The instantaneous partial tool working part deflection $y_d(t)$ can be calculated from the differential motion equation:

$$m \cdot \ddot{y}_d(t) + c \cdot \dot{y}_d(t) + k \cdot y_d(t) = F_{fNe}(t) \tag{5}$$

In the first step, the left side of equation (5) has to be identified. In order to determine modal parameters (m, c, k), an impact test should be carried out. Considering the right hand side of equation (5) it was assumed that instantaneous tool deflections are a consequence of instantaneous cutting

forces affected by the value of static run out e_r. The instantaneous feed normal force $F_{fNe}(t)$ including static run out is expressed by:

$$F_{fNe}(t) = \left(k_c \cdot \cos\varphi - k_{cN} \cdot \sin\varphi\right) \sum_{i=1}^{z_c} A_{Dze} \tag{6}$$

where:, A_{Dze} denotes active sectional area of the cut including static run out, φ is the instantaneous angular position of the cutting edge, k_c, k_{cN} are specific cutting pressures and z_c is the active number of teeth. k_c, k_{cN} can be determined from the calibration tests.

The instantaneous angular position of the cutting edge φ is formulated as the average angle between the starting angle φ_1 and finishing angle φ_2 of the cutting edge (see figure 2) ($\varphi = (\varphi_2 - \varphi_1)/2$).

The active sectional area of the cut including static run out can be calculated from the following equation:

$$A_{Dze} = \frac{f_{ze} \cdot R}{\sin\lambda_s}\left(\cos\varphi_1 - \cos\varphi_2\right) \tag{7}$$

where: f_{ze} is the feed per tooth including static run out.

The z_c parameter denotes the number of teeth which are contacted with the work piece during cutting, in the range of the specified working angle ψ. The active number of teeth for a cylindrical milling cutter with helical cutting edges ($\lambda_s \neq 0$) can be expressed as:

$$z_c = \frac{\psi \cdot z}{2\pi} + \frac{a_p \cdot z \cdot \tan\lambda_s}{2\pi \cdot R} \tag{8}$$

where: z is the number of teeth.

Feed per tooth including static run out can be determined from the following equation:

$$f_{ze} = f_z - \frac{y_r(t)}{2\sqrt{\frac{2a_e}{R}\left(1 - \frac{2a_e}{R}\right)}} \tag{9}$$

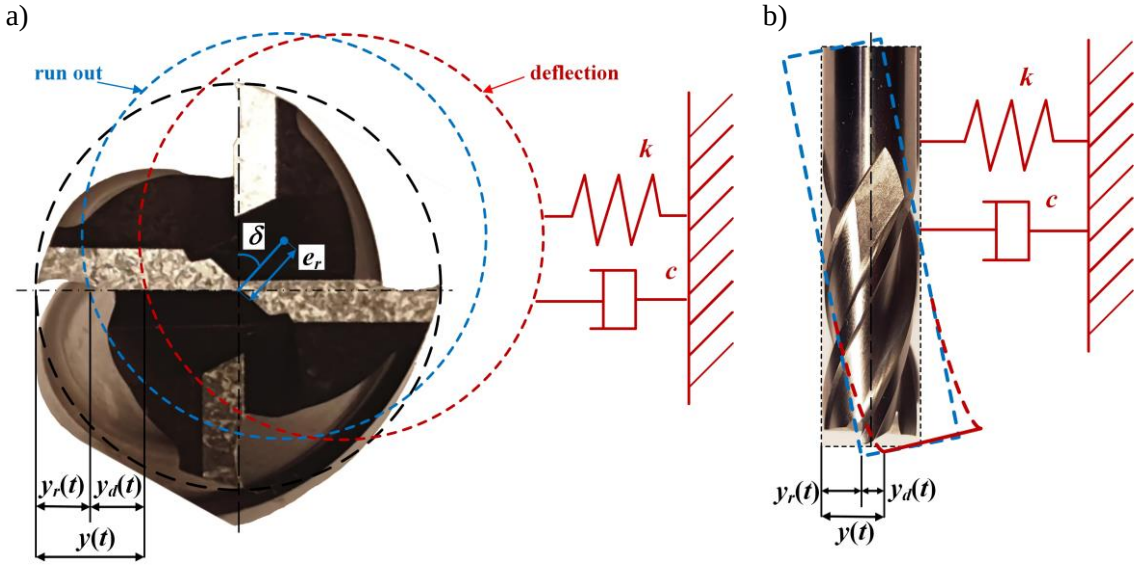

Fig. 1. Cylindrical end mill displacements during machining: a) face of the cutter; b) reference plane

Calculation of the active sectional area of cut requires the determination of boundary conditions (i.e. φ_1, φ_2 values). During cylindrical down milling, when the condition: $a_p > (\psi R)/(\tan \lambda_s)$ is fulfilled, three phases of tool immersion into the work-piece can be distinguished as a function of tool rotation angle Ω (Fig. 2).

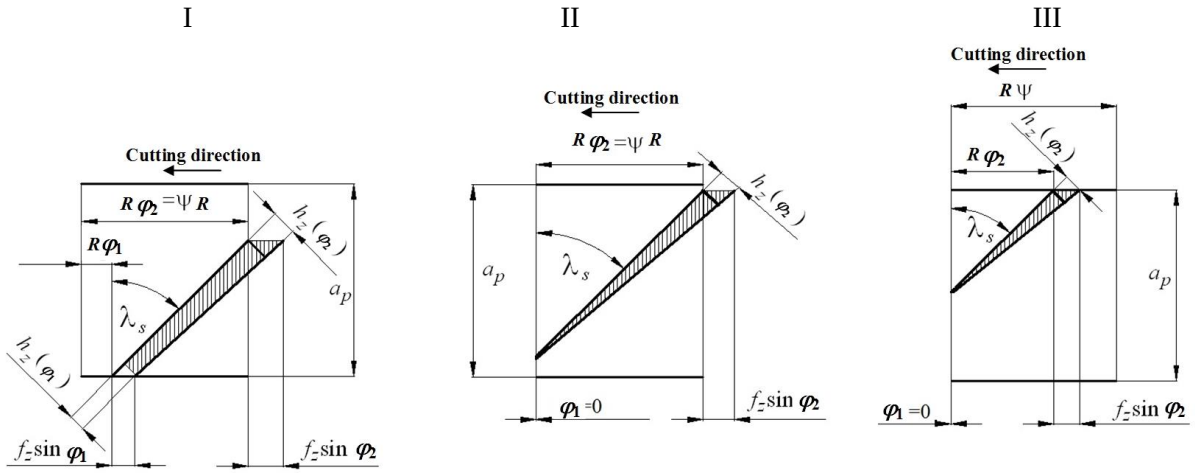

Fig. 2. Developed view of the contact area between the tool and work piece during milling

These phases can be described mathematically as:

Phase 1:

$$\frac{\pi}{2}-\psi+\frac{2\pi}{z}(i-1)+2\pi(N-1)\le\Omega<\frac{\pi}{2}+\frac{2\pi}{z}(i-1)+2\pi(N-1) \tag{10}$$

$$\varphi_1=\frac{\pi}{2}-\Omega-\frac{2\pi}{z}(i-1)+2\pi(N-1)\quad \varphi_2=\psi=\arccos\left(1-\frac{a_e}{R}\right) \tag{11}$$

Phase 2:

$$\frac{\pi}{2}+\frac{2\pi}{z}(i-1)+2\pi(N-1)\le\Omega<\frac{a_p\cdot\tan\lambda_s}{R}+\frac{\pi}{2}-\psi+\frac{2\pi}{z}(i-1)+2\pi(N-1) \tag{12}$$

$$\varphi_1=0\quad \varphi_2=\psi \tag{13}$$

Phase 3:

$$\frac{a_p\cdot\tan\lambda_s}{R}+\frac{\pi}{2}-\psi+\frac{2\pi}{z}(i-1)+2\pi(N-1)\le\Omega<\frac{a_p\cdot\tan\lambda_s}{R}+\frac{\pi}{2}+\frac{2\pi}{z}(i-1)+2\pi(N-1) \tag{14}$$

$$\varphi_1=0\quad \varphi_2=\frac{\pi}{2}+\frac{a_p\cdot\tan\lambda_s}{R}-\Omega-\frac{2\pi}{z}(i-1)+2\pi(N-1) \tag{15}$$

where: i is the ordinal number of tooth and N is the number of tool rotations.

Representative partial – $y_r(t)$, $y_d(t)$ and total – $y(t)$ milling tool working part displacements, calculated on the basis of equations (1, 2 and 5) are presented in Figure 3. It can be observed that the total displacement $y(t)$ is characterized by the appearance of an envelope which has a period equal to the tool revolution time. According to previous research [17], the maximum height of this envelope $y_{e\max}$ contributes directly to the machined surface profile. The height of this displacement envelope $y_{e\max}$ results from the static run out and dynamic phenomena occurring in machining process. The static run out e_r can be induced by the tool wear, cutting edge asymmetry, insert setting, dynamic

imbalance and thermal deformation. However, the main reason for its occurrence is the offset between the position of the tool rotation axis and the spindle axis.

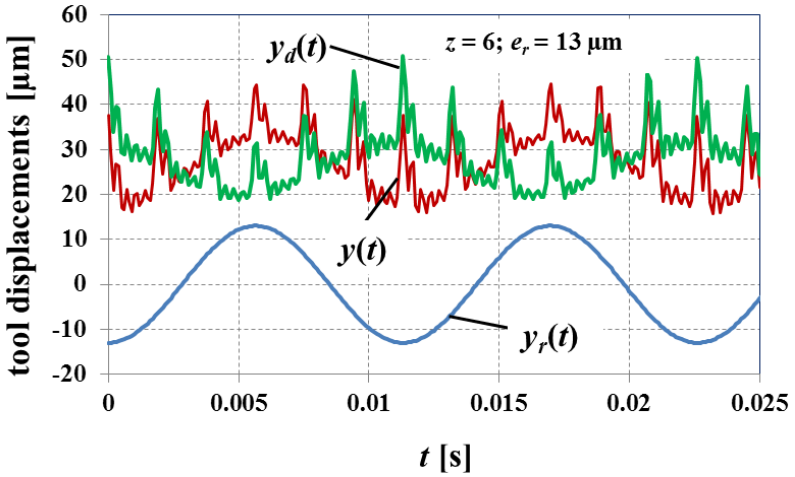

Fig. 3. Modeled cylindrical milling tool working part displacements: $y_r(t)$, $y_d(t)$, $y(t)$

The proposed surface roughness model indicates that during cylindrical milling, two different mechanisms of surface profile formation can occur (Fig. 4). Their appearance is dependent on the relation between the selected feed per tooth f_z value and the critical feed per tooth value $f_{z\ cr.}$ (Fig. 4a). The $f_{z\ cr.}$ value can be obtained on the basis of equation:

$$f_{zcr.} = \sqrt{y_{e1}\left(2R - y_{e1}\right)} \tag{16}$$

The y_{e1} parameter in equation (16) denotes the partial displacement between the two consecutive teeth. Assuming that partial displacements are equal for all teeth, then: $y_{e1} = 2y_{emax}/z$. When $f_z < f_{z\ cr.}$ (i.e. for small values of feed per tooth and/or large values of cutter displacement y_{emax}) then surface asperities are removed by subsequent tooth positions (see – Fig. 4b) and the surface roughness height is lower than the height of the cutter displacement envelope y_{emax} – which is highly desirable. Surface roughness height for $z = 6$ can be obtained from the following expression:

$$Rt\left(y_{emax}\right) = \frac{y_{emax}}{3} + R - \sqrt{R^2 - 4{f_z}^2} \tag{17}$$

When the $f_z \geq f_{z\ cr.}$ (i.e. for larger values of feed per tooth and/or smaller values of cutter displacement envelope height) surface asperities are at least equal to y_{emax} (see – Fig. 4c), and they are not removed by the trajectories of the subsequent teeth. In this case, surface roughness height can be calculated from the following equation:

$$Rt(y_{emax}) = \frac{2\left(4{y_{emax}}^2 + f_z^2 \cdot z^2\right)\cdot\left(y_{emax}\cdot z\right) - f_z \cdot z \cdot \sqrt{4{y_{emax}}^2 + f_z^2 \cdot z^2}\cdot\sqrt{z^2\left(4R^2 - f_z^2\right) - 4{y_{emax}}^2}}{2z\cdot\left(4{y_{emax}}^2 + f_z^2 \cdot z^2\right)} -$$
$$- \frac{2\left(4{y_{emax}}^3 - 4R\cdot{y_{emax}}^2\cdot z + f_z^2 \cdot y_{emax}\cdot z^2 - f_z^2 \cdot R \cdot z^3\right)}{2z\cdot\left(4{y_{emax}}^2 + f_z^2 \cdot z^2\right)}, \tag{18}$$

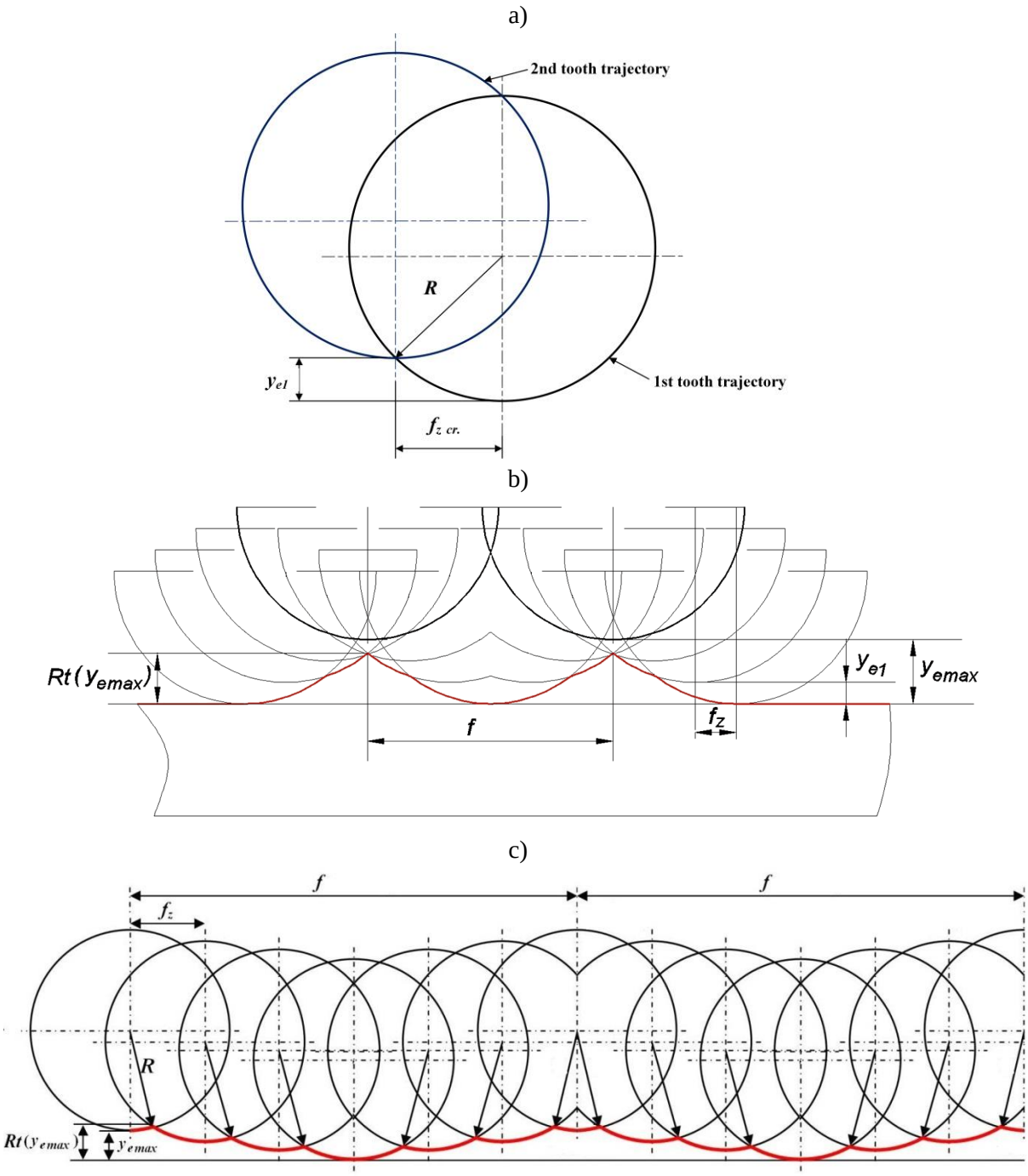

Fig. 4. Surface profile model including the height of cutter displacement envelope: a) designation of the critical feed per tooth $f_{z\,cr}$; b) when the $f_z < f_{z\,cr.}$; c) when the $f_z \geq f_{z\,cr.}$

3 MATERIAL AND METHODS

Experimental investigations were carried out on hardened hot-work tool steel (55NiCrMoV6, hardness approx. 55 HRC). A monolithic cylindrical end mill (z = 6, D = 12 mm diameter, r_ε = 1 mm corner radius, λ_s = 45°, orthogonal rake angle γ_o = -15°, orthogonal flank angle α_o = 6°) was selected. The cutting edges were made from fine-grained sintered carbide (mean grain size approx. 0.4 μm) with TiAlN coating. Experiments were conducted in down milling conditions on a 5-axes CNC milling workstation (DECKEL MAHO DMU 60monoBLOCK) with maximumal rotational speed of

24 000 rev/min and maximumal power of 26 kW. Cutting parameters applied in the research are presented in the Table 1.

Table 1. Design of experiment

Feed per tooth f_z [mm/tooth]	Cutting speed v_c [m/min]	Rotational speed n [rev/min]	Axial depth of cut a_p [mm]	Radial depth of cut a_e [mm]
0.1; 0.12; 0.14; 0.18	300	7958	3; 6.3; 7	0.2; 0.5

Tool displacements $y(t)$ were measured using a laser vibrometer for f_z =0.1 mm/tooth. In all investigated instances tool wear per tooth was VB_B < 0.05 mm. Surface roughness measurements were made using a T500 portable stylus surface profiler (Hommelwerke), equipped with T5E head and Turbo DATAWIN software. The sampling length lr = 0.8 mm, the evaluation length ln = 5·lr = 4.0 mm, the length of cutoff wave λc = 0.8 mm and an ISO 11562(M1) filter were applied. Using the surface profile charts obtained, the *Ra* and *Rz* parameters (according to ISO 4287:1984) were calculated using Turbo DATAWIN software. Measurements for each investigated cutting speed value were repeated 3 times in order to calculate the mean arithmetic value of *Ra* and *Rz* parameters. In order to solve the differential motion equation (5), modal parameters (m, c, k) were determined using an impact test [5], giving the following parameters: m = 0.079 Ns^2/m, c = 40.8 Ns/m, k = 19492469 N/m. Specific cutting pressures k_c, k_{cN} appearing in equation (4) were obtained from calibrations tests as: k_c = 4869,5 $h_z^{-0,34}$ [MPa] and k_{cN} = 0,0003 $h_z^{-3,5}$[MPa]. The calibration method used is described in detail in [21]. The differential motion equation (5) was solved in **Simulink** software equipped with **ode45** solver. The developed displacements model is shown schematically in Figure 5.

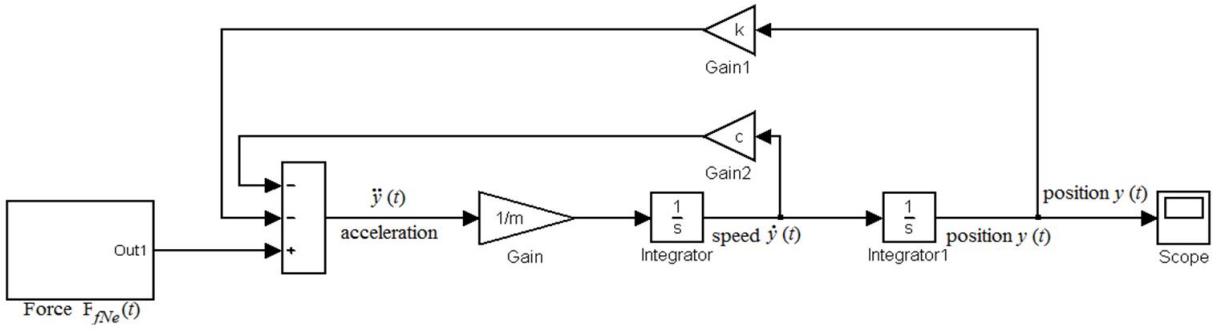

Fig. 5. Model of cutter's displacements developed in Simulink software

In order to measure cutter displacements during the milling process a scanning laser vibrometer (Polytec PSV-400) was used (Fig. 6). The sampling frequency of 50 kHz was selected. Cutter displacement measurements were conducted in the feed normal direction, and taken from the end of the tool shank (at the distance l_m from the collet, see Figure 6), because it is impossible to conduct the measurement on the working part of tool during milling. These tool displacement signals as functions of time, measured using the laser vibrometer, consist of many constituents, and hence the identification of those related to dynamic cutter run out is complex. Therefore, the spectrum of the displacement signals was analysed using Fast Fourier Transform (FFT). Furthermore, the software low-pass Chebyshev's filter was applied in order to eliminate the undesirable constituents of the signal. The maximum cutter displacement per one tool revolution, can be determined from the measured displacements using the following equation, assuming that the cutter can be treated as a cantilever beam:

$$y_{e\max} = 2\left[e_r + \left(\left(y(f_o) + y(zf_o - f_o) + y(zf_o + f_o) + y(2zf_o - f_o) + y(2zf_o + f_o)\right) - \frac{e_r \cdot l_m}{l}\right) \cdot \frac{2l^3}{l_m^2(3l - l_m)}\right] \quad (19)$$

where: $y(f_o)$, $y(zf_o\text{-}f_o)$, $y(zf_o\text{+}f_o)$, $y(2zf_o\text{+}f_o)$, $y(2zf_o\text{-}f_o)$ are the measured amplitudes of the cutter's displacement from the FFT analysis, l = tool overhang, l_m = distance from the collet to the measurement point.

Equation (19) enables the estimation of the y_{emax} for the tool tip, considering deflection induced by cutting forces and tool axis tilting (induced by the geometrical errors of machine - tool-holder - tool system). Cutter static run out parameters were measured offline using a dial indicator on the working part of the tool. The obtained values were: e_r=13 µm, δ=0°. It should be noted that the static maximum cutter displacement for one tool revolution is equal to $2e_r$.

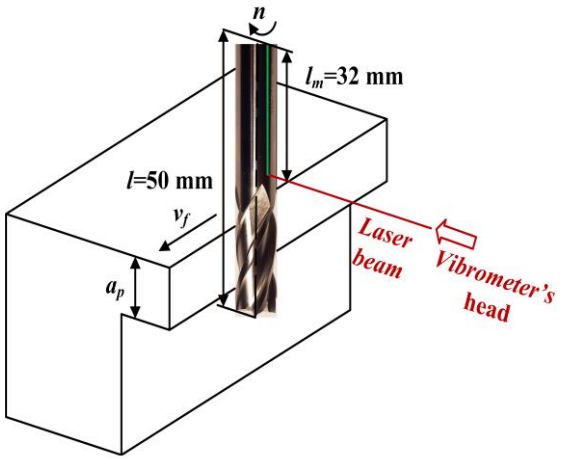

Fig. 6. The scheme of tool's displacement measurement with laser vibrometer

4 RESULTS AND DISCUSSIONS

Figures 7 to 9 depict the simulated (based on equation 1) and measured (using laser vibrometer) cutter displacements in the time domain. It can be seen that the simulated and measured displacements are similar, both in a quantitative and qualitative sense. In figures 7 and 8 the displacement's wavelength corresponds directly to feed per tooth value f_z and $z{\cdot}f_o$ frequency (number of teeth multiplied by spindle rotational frequency). This indicates that it is caused by cutting forces generated in the milling process. However, this is not the case with the results presented in Figure 9. The differences result from the selection of cutting parameters, which – for the case presented in Figure 9 – fulfill the condition of milling force consistency (when a_p = 6.3 mm and a_e = 0.2 mm, the axial depth of cut to axial pitch is: a_p / p_o = 1). Thus, the cutting force generated during milling is almost constant and the tool's displacements are mainly caused by the occurrence of run out. From figures 7 and 8 it can also be seen that maximum instantaneous displacement values for consecutive teeth are not uniform. Variations of these instantaneous maximum displacements produce an envelope which has a period equal to the tool revolution time and is essentially sinusoidal. This displacement envelope y_e is induced mainly by cutter's radial run out e_r. Figures 7 to 9 show some discrepancies between the measured and calculated displacements. These probably result from the method of measurement, which was carried out on the joining part of the tool (at the distance l_m from the collet), instead of the tool's working part, as well as filtration of the measured displacement signal.

Figure 10 depicts the spectrum analysis of the simulated (Fig. 10a) and measured (Fig. 10b) cutter displacements, based on Fast Fourier Transform (FFT). These spectra have a similar form. In both spectra the displacement signal consists of constituents at the tooth passing frequency zf_o, and its first harmonics $2zf_o$, which are induced by cutting forces. However, the spectra also contain components

with the following frequencies: f_o, zf_o- f_o, zf_o+ f_o, $2zf_o$- f_o, $2zf_o$+ f_o which are related to the appearance of radial run out.

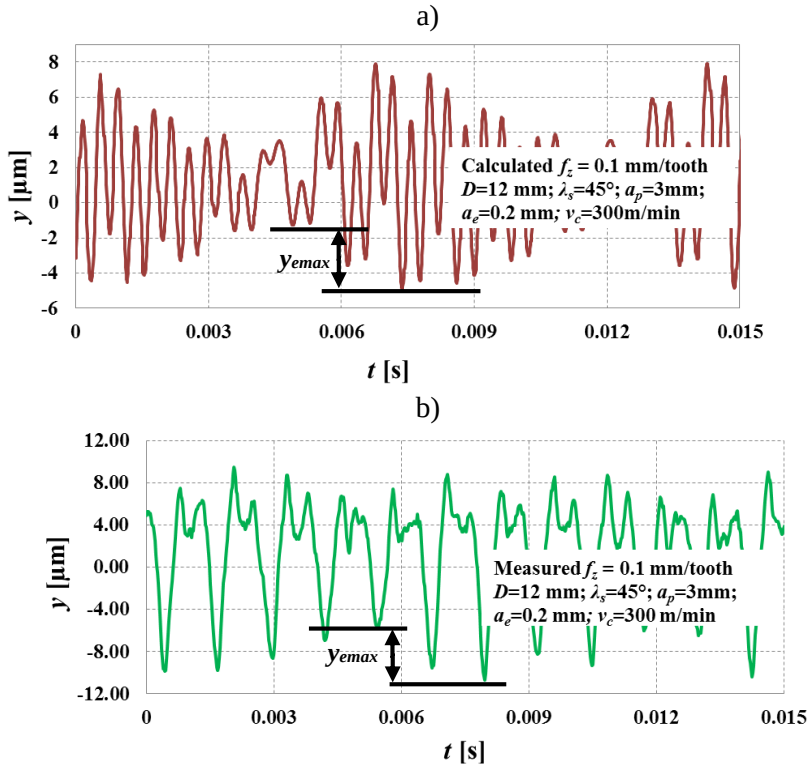

Fig. 7. The time course of cutter's displacement for a_p = 3 mm, a_e = 0.2 mm: a) simulated, b) measured

Figure 11a shows the measured and calculated values of the cutter displacement envelope height y_{emax}. It was found, that for a_p = 3 mm and a_e = 0.2 mm, the maximum cutter displacements obtained from the developed model and measurements using laser vibrometer were significantly smaller than those resulting from static run out ($2e_r$) alone. However, these differences reduce as cutting depth increases. Figure 11a also shows that the values of y_{emax} obtained from the developed model are in good agreement with those measured using the laser vibrometer.

Figures 11b and 11c show the surface roughness parameters *Ra* and *Rz* measured with the surface profiler, calculated on the basis of the traditional kinematic-geometric model (*Rzt*, *Rat*), and estimated using the proposed model with static displacements $Rt(2e_r)$, $Ra(2e_r)$ and dynamic displacements $Rt(y_{emax})$, $Ra(y_{emax})$. The $Rt(2e_r)$ and $Ra(2e_r)$ values were determined from equation (17) with the assumption that the cutter's displacement envelope height is caused only by static radial run out: y_{emax} = $2e_r$. The $Rt(y_{emax})$ and $Ra(y_{emax})$ values were calculated from equations (17) and (18) with y_{emax} values obtained from the total tool displacement model (see – equation 1).

It can be seen that surface roughness parameters' *Rz* values calculated using the dynamic displacement model are similar to those measured using the surface profiler, independent of feed per tooth value (Fig. 11b).

a)

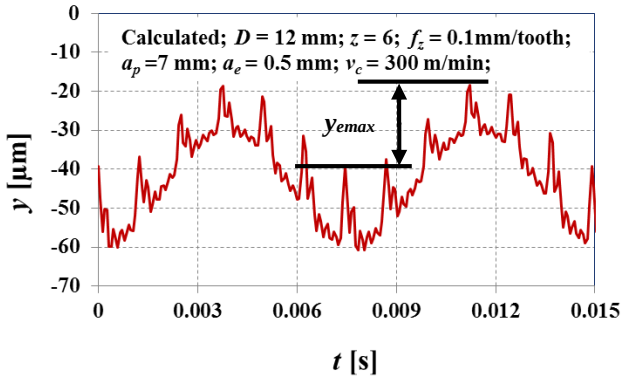

b)

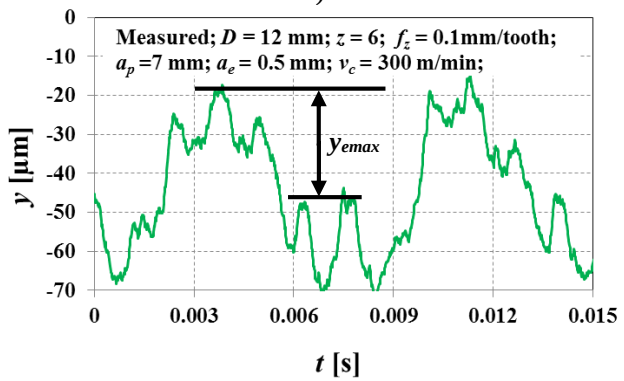

Fig. 8. The time course of cutter's displacement for a_p = 7 mm, a_e = 0.5 mm: a) simulated, b) measured

a)

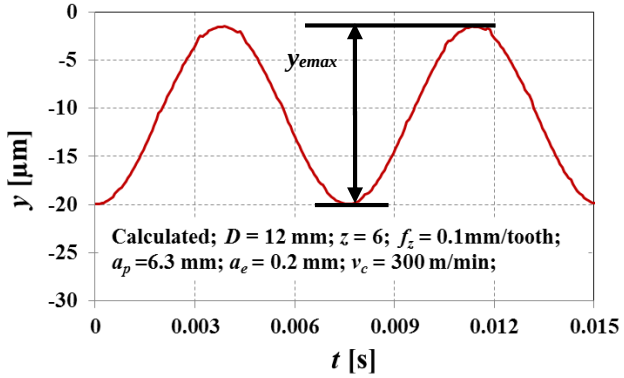

b)

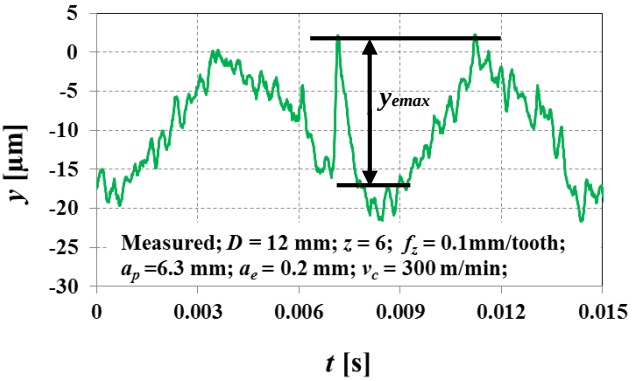

Fig. 9. The time course of cutter's displacement for a_p = 6.3 mm, a_e = 0.2 mm: a) simulated, b) measured

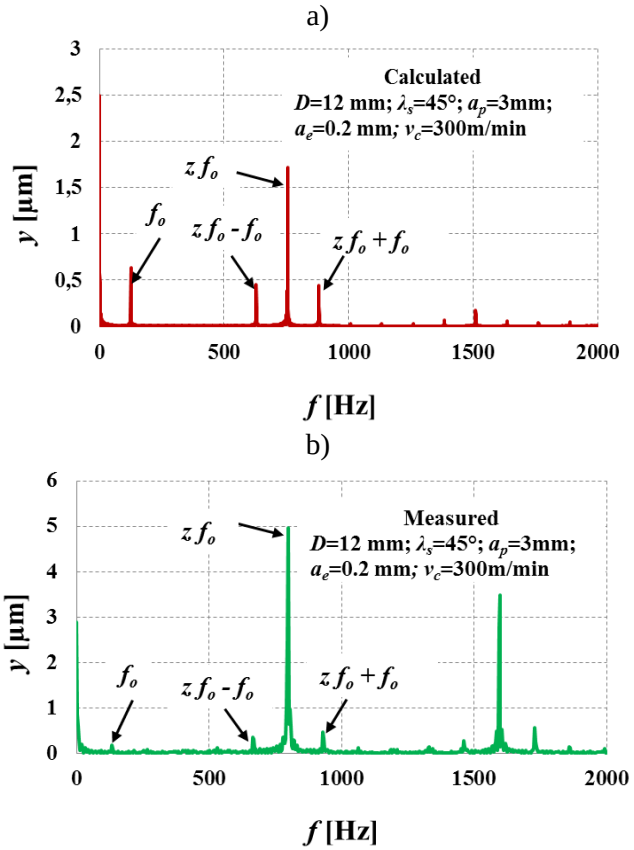

Fig. 10. FFT spectra of cutter's displacement: a) simulated, b) measured

Simulations have revealed that for f_z = 0.14 mm/tooth, $f_z \geq f_{z\,cr}$. Therefore, for lower values of feed per tooth (f_z < 0.14 mm/tooth), surface roughness was calculated from equation (17), while for the higher feed per tooth values (f_z = 0.14, 0.18 mm/tooth) *Rz* parameter was calculated from equation (18).

Figure 11c compares the measured and modeled average surface roughness height values, *Ra*. In order to calculate the theoretical average surface roughness it was assumed that: $Ra(y_{emax}) = Rt(y_{emax})/5$ and $Ra(2e_r) = Rt(2e_r)/5$. Figure 11c shows that $Ra(y_{emax})$ values are comparable to the measured ones (with one exception for the f_z = 0.12 mm/tooth). Therefore, the proposed model based on dynamic displacements can be also successfully applied to the estimation of the average surface roughness height. However, the surface roughness parameters determined on the basis of static displacements ($Rt(2e_r)$, $Ra(2e_r)$) overestimate the measured values. This is caused by the significantly higher value of cutter displacement envelope height resulting from static run out than that measured with laser vibrometer (see – Fig. 11a). This observation indicates that during cylindrical end milling, surface roughness can be strongly affected by the simultaneous effect of static run out and dynamic tool deflections caused by cutting forces. It should be also noticed that theoretical surface roughness values *Rat* and *Rzt* resulting from the kinematic-geometric model are significantly lower than the measured *Ra* and *Rz* values.

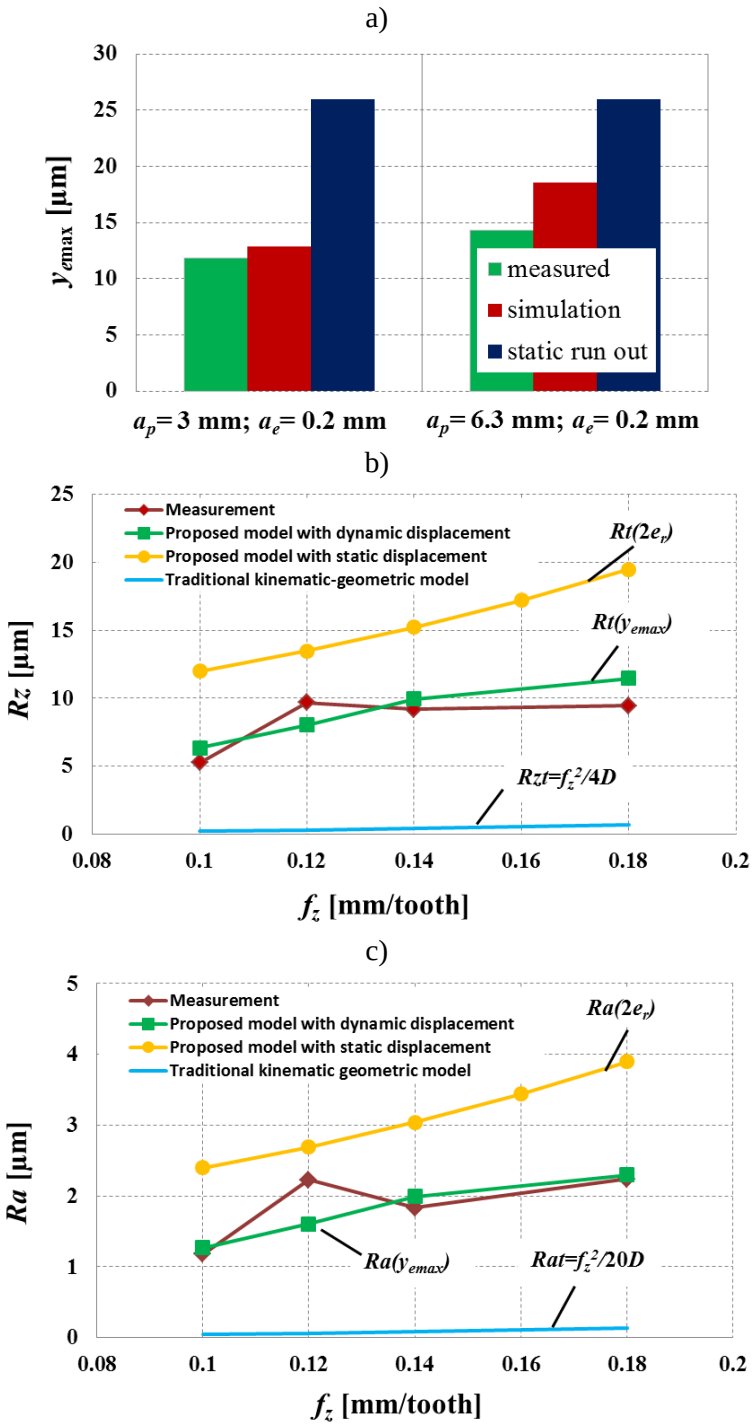

Fig. 11. The comparison of measured and calculated values (a_p = 3 mm) of: a) height of cutter's displacement envelope y_{emax}, b) surface roughness *Rz*, c) surface roughness *Ra*

5 CONCLUSIONS

This paper was concerned with the modeling of surface roughness during cylindrical milling using a model based on tool displacement. The proposed approach included the influence of cutting parameters, tool static run out, and deflections induced by cutting forces. Based on the experimental observations, the following conclusions have been reached:

1. A cylindrical milling tool's displacements during finish milling of hardened steel are induced by radial run out which results from geometrical errors, as well as dynamic deflections caused by forces generated during machining. Cutter displacement values obtained from the developed dynamic model are in good agreement with the measured ones, both in quantitative and qualitative aspects. The FFT spectra of the calculated and measured displacement signals consist of the same constituents which confirms the validity of the model.
2. The maximum cutter displacement envelope height determined from the developed model and experimental measurements typically have a different value to that resulting from the static run out ($2e_r$) measurement. This shows that during milling, cutting forces induce a dynamic cutter run out, which differs from the static run out. Thus, a reliable surface profile model for cylindrical milling must include the dynamic behaviour during machining.
3. The surface roughness values *Ra*, *Rz* estimated on the basis of the developed model including dynamic cutter displacement are in good agreement with measured values over a range of feed per tooth values. The agreement between the measured and calculated surface roughness values are in the range of 80-92% for *Rz* and 61-98% for *Ra*.
4. The agreement between the measured and calculated surface roughness (*Ra*, *Rz*) parameters in the range of feed per tooth values investigated indicates that in the cylindrical milling process two different mechanisms of surface irregularity formation can appear. The occurrence of these mechanisms depends on the relative values of the feed per tooth value and the height of the cutter displacement envelope. However, a more comprehensive understanding of these mechanisms requires further studies focusing on the precise measurements of machined surface topographies.
5. The application of a model which included only the effect of static displacements typically had a lower accuracy than the dynamic model. In that case the agreement between the measurements and model did not exceeding 72% for *Rz* and 83% for *Ra*.

6 REFERENCES

[1] Urbanski JP, Koshy P, Dewes RC, Aspinwall DK. High speed machining of moulds and dies for net shape manufacture. Materials and Design 2000;21:395–402.

[2] Wojciechowski S. The estimation of cutting forces and specific force coefficients during finishing ball end milling of inclined surfaces. International Journal of Machine Tools & Manufacture 2015;89:110–23.

[3] Ruggiero A, D'Amato R, Gómez E, Merola M. Experimental comparison on tribological pairs UHMWPE / TIAL6V4 alloy , UHMWPE / AISI316L austenitic stainless and UHMWPE / AL_2O_3 ceramic, under dry and lubricated conditions. Tribology International 2016;96:349–360.

[4] Ruggiero A, D'Amato R, Gómez E. Experimental analysis of tribological behavior of UHMWPE against AISI420C and against TiAl6V4 alloy under dry and lubricated conditions. Tribology International 2015;92:154–161.

[5] Twardowski P, Wojciechowski S, Wieczorowski M, Mathia T. Surface roughness analysis of hardened steel after high-speed milling. Scanning 2011;33:386–95.

[6] Kumar R, Chattopadhyaya S, Hloch S, Krolczyk GM, Legutko S. Wear characteristics and defects analysis of friction stir welded joint of aluminium alloy 6061-T6. Eksploatacja i Niezawodnosc – Maintenance and Reliability 2016:18:128–135.

[7] Jozwik J, Mika D. Diagnostics of workpiece surface condition based on cutting tool vibrations during machining. Advances in Science and Technology Research Journal 2015;9:57–65.

[8] Baek DK, Ko TJ, Kim HS. Optimization of feedrate in a face milling operation using a surface roughness model. International Journal of Machine Tools & Manufacture 2001;41:451–62.

[9] Li SJ, Liu RS, Zhang AJ. Study on an end milling generation surface model and simulation taking into account of the main axle's tolerance. Journal of Materials Processing Technology 2002;129: 86-90.
[10] Franco P, Estrems M, Faura F. A study of back cutting surface finish from tool errors and machine tool deviations during face milling. International Journal of Machine Tools & Manufacture 2008;48:112–23.
[11] Buj-Corral I, Vivancos-Calvet J, Gonzalez-Rojas H. Influence of feed, eccentricity and helix angle on topography obtained in side, milling processes. International Journal of Machine Tools & Manufacture 2011;51:889–97.
[12] Baek DK, Ko TJ, Kim HS. A dynamic Surface roughness model for face milling. Precision Engineering 1997;20:171–8.
[13] Zhenyu S, Luning L, Zhanqiang L. Influence of dynamic effects on surface roughness for face milling proces. International Journal of Advanced Manufacturing Technology 2015;80:1823–31.
[14] Peigne G, Paris H, Brissaud D, Gouskov A. Impact of the cutting dynamics of small radial immersion milling operations on machined surface roughness. International Journal of Machine Tools & Manufacture 2004;44:1133–42.
[15] Liu X, Cheng K. Modelling the machining dynamics of peripheral milling. International Journal of Machine Tools & Manufacture 2005;45:1301–20.
[16] Schmitz TL, Couey J, Marsh E, Mauntler N, Hughes D. Runout effects in milling: Surface finish, surface location error, and stability. International Journal of Machine Tools & Manufacture 2007;47:841–51.
[17] Wojciechowski S. Machined surface roughness including cutter displacements in milling of hardened steel. Metrology and Measurement Systems 2011;XVIII:429–40.
[18] Tatar K, Gren P. Measurement of milling tool vibrations during cutting using laser vibrometry. International Journal of Machine Tools & Manufacture 2008;48:380–7.
[19] Miyaguchi T, Masuda M, Takeoka E, Iwabe H. Effect of tool stiffness upon tool wear in high spindle speed milling using small ball end mill. Precision Engineering 2001;25:145–54.
[20] Wojciechowski S, Chwalczuk T, Twardowski P, Krolczyk GM. Modeling of cutter displacements during ball end milling of inclined surfaces. Archives of Civil and Mechanical Engineering 2015;15:798–805.
[21] Jayaram S, Kapoor SG, DeVor RE. Estimation of the specific cutting pressures for mechanistic cutting force models. International Journal of Machine Tools & Manufacture 2001;41:265–81.